Project Report for Master of Engineering

Stabilization plan of inkjet process through evaluation of rheological properties

유변특성 평가를 통한 잉크젯 공정 안정화 방안

February 2021

Seoul National University
Graduate School of Engineering Practice
Yong-Hyun Jin

Stabilization plan of inkjet process through evaluation of rheological properties

Advisor: Kyung-Hyun Ahn

Submitting a Master's Project Report

February 2021

Seoul National University

Graduate School of Engineering Practice

Yong-Hyun Jin

Confirming the master's Project Report

written by Yong-Hyun Jin

February 2021

Chair	Hwa-Yong Kim	(Seal)
Examiner	Kwang-Sup Jung	(Seal)
Examiner	Kyung-Hyun Ahn	(Seal)

NOTICE

This project report includes the contents of papers that we published while researching at the Graduate School of Engineering Practice, Seoul National University.

1. Yong-Hyun Jin, Kyung-Hyun Ahn ”Stabilization plan of inkjet process through evaluation of rheological properties,” Summer Annual Conference of IEIE, pp. 2375-2377, 2020.

Abstract

Stabilization plan of inkjet process through evaluation of rheological properties

Yong-Hyun Jin
Graduate School of Engineering Practice
Seoul National University

Recently, display products have been diversified into product forms such as bending or folding screen, and the panel gets thin and large to reflect the needs of consumers. To meet the needs of these customers, the cost of products is gradually increasing as manufacturers are using expensive equipment applying the latest technology. Accordingly, the display industry is striving to improve the existing costly production process to a low-cost process by applying alternative technologies. Among the OLED[1] display production techniques, the deposition process needs the most improvement. There is an urgent need for improvement due to high equipment maintenance costs and waste of organic material. Consequently, the industry is paying attention to inkjet printing as a new technology that replaces the current deposition process, and the production cost can be reduced by 50% or more when applying inkjet. However, since there is no standard in the inkjet process, it is difficult for developers to take inkjet the process.

[1] Organic Light Emitting Diode

Therefore, this study focuses on the stabilization of the inkjet printing process by applying a suspension analysis method based on rheological properties. Based on the fact that the process results vary depending on the rheological properties of the suspension, the correlation between the rheological properties of various paints and the contact angle of samples was analyzed. It was found that the viscosity is increased with increasing contact angle. And additional experiments were conducted using a suspension with PMMA[2] particles. It was confirmed that the viscosity is increased with the volume fraction increased. We also found that increasing the particle volume fraction up to 15% can increase the viscosity value up to 100%.

Through these studies, we established an inkjet process stabilization methodology using the relationship between the rheological properties and the inkjet display. Using this, we laid the foundation for the company's inkjet process SOP[3].

Keywords : inkjet printing, stabilization plan, Rheological property evaluation, viscosity/contact angle, silicone oil/PMMA suspension

Student Number : 2019-26873

[2]Poly methyl methacrylate
[3]Standard Of Procedure

Contents

List of Figures

List of Table

Chapter 1

Introduction

1.1 Background and motivation

Recently, electronic product gets thinner and larger after reflecting consumer needs. Display products follow similar trend, and the production cost is gradually increasing as the form factor changes to be foldable. Therefore, for economic competitiveness against competitors, display industries have been developing technology to improve the productivity by increasing the size of production glass up to 10.5G[1] as shown in the Figure 1.1[2].

The display industry can be largely divided into LCD[3] and OLED[4]. Among the two industries, the OLED-related industry shows a strong will to increase the size and apply alternative technology. The reason for this is that in the case of LCDs, production technologies have already been enlarged/advanced, and production processes have been optimized, so the cost of producing products is considerably lower compared to OLED. The representative process required for OLED product production can be divided into 4 steps as shown in the Figure 1.2[5]. There is a back-plane process in which the surface of a substrate is crystallized with a laser, and a driving element TFT and various wiring are formed, and there is an evaporation process in which organic material is boiled and attached to the substrate to form a pixel that emits light.

[1] Glass size Generation
[2] Source: Samsung display news-room
[3] Liquid Crystal Display
[4] Organic Light Emitting Diode
[5] Source: Electronic components research institute

The encapsulation process in which metal or inorganic material is covered to protect the device on the finished surface and lastly, there is a module process in which driving part is attached to the production substrate and defects are checked to finish product. Among these four-step processes, the process that desperately needs to reduce equipment maintenance costs or material costs is the evaporation process in which organic materials are attached to the substrate. The organic material evaporation process equipment is imported exclusively from Japan, and the equipment price and maintenance cost are very high because the equipment needs to be kept in a vacuum. And evaporation process using mask wastes more than 30% of the materials as shown in the Figure 1.3[6].

For this reason, the OLED manufacturers are trying to secure the cost competitiveness by reducing equipment costs and efficient use of material by introducing alternative technologies for the evaporation process. Among the recent alternative technologies, inkjet printing technology is unique. When the technology is introduced, it can change from vacuum equipment with low material efficiency and high equipment and operating costs to liquid atmospheric equipment with high material efficiency and low equipment and operating costs. Then, as shown in the Table 1.1, the process is simplified, reducing equipment costs and improving material efficiency, which can reduce production costs. The effect of this technology development has been confirmed by DuPont's press release as shown in the Figure 1.4[7]. When using the inkjet process, the cost of 55-inch OLED TV panels can be reduced by 30% compared to LCD and by half compared to current OLED. For this reason, for the introduction of inkjet printing technology, developers are conducting process tests by manufacturing special suspensions containing organic particles and printing equipment, but there are

[6]Source: Samsung display news-room
[7]Source: DuPont press release

no process specifications or standardized procedures.

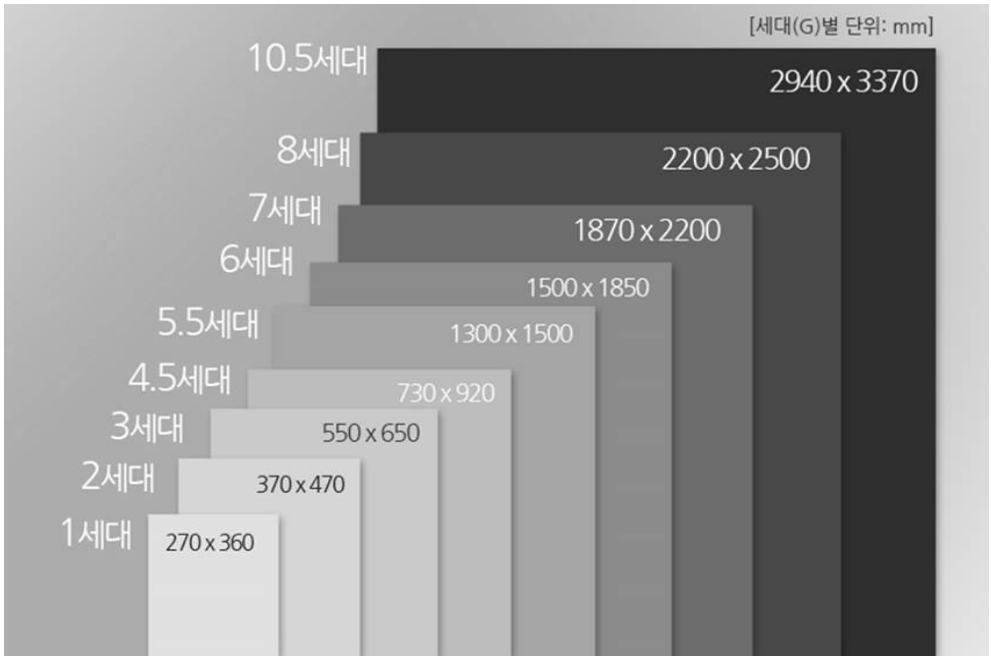

Figure 1.1: Display generation and size

Table 1.1: Characteristics and process comparison by an OLED manufacturing method

Item	RGB OLED	White OLED	Inkjet OLED
Method	Evaporation	Evaporation	Printing
Mask	FMM	Open	-
Pixel structure	RGB	Overlay	RGB
Color filter	-	Need	-
8th Gen	Hard	Normal	Normal
Material efficiency	Bad	Normal	Good
Manufacturing price	High	High	Low

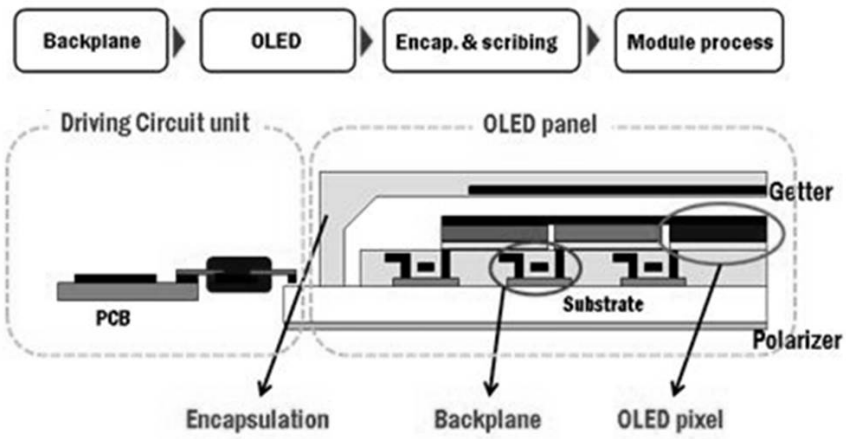

Figure 1.2: OLED composition and process sequence

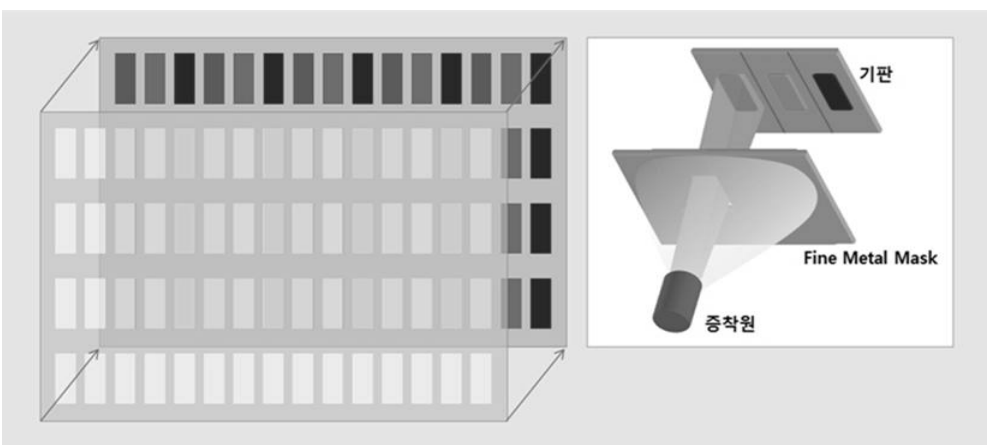

Figure 1.3: OLED device evaporation using a fine metal mask

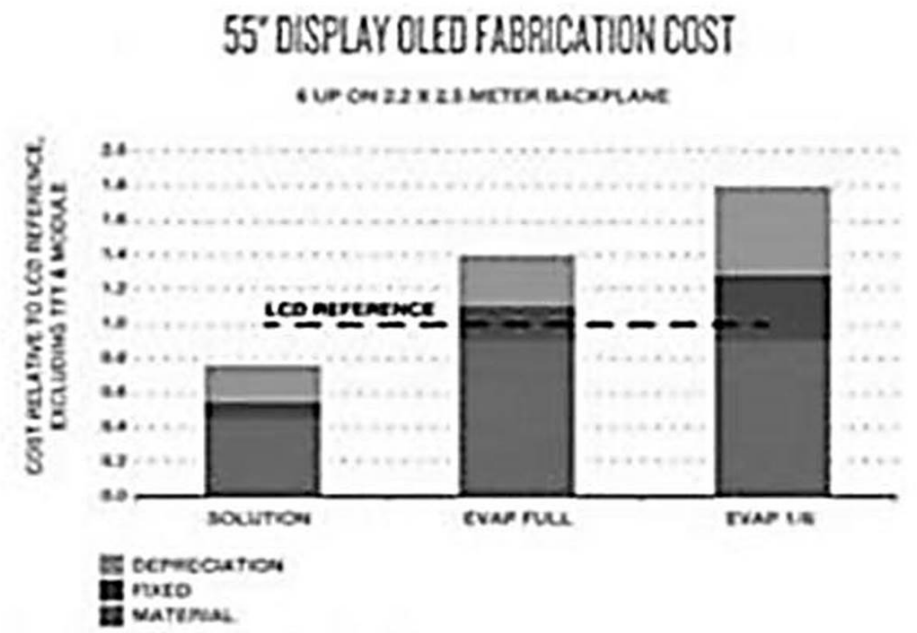

Figure 1.4: Production cost comparison(LCD, Evaporation, Inkjet)

1.2 Object of the thesis

The main purpose of this study is to significantly reduce the stabilization time of the inkjet printing process under development. Currently, stabilization is carried out by directly putting it into the equipment without analyzing inkjet materials, but we are trying to propose a faster and more systematic process stabilization method by analyzing the correlation between the rheological properties of the suspension material containing organic particles and the process performance. Specifically, by analyzing the rheological properties of the ink and product performance, it is desirable to find and use rheological properties that influence process results. Using this, we are going to build an optimized SOP[8] that uses specific rheological properties as a standard for setting process stabilization of the equipment when a new suspension is introduced in the future.

Thus, in this study, the correlation between the rheological properties of various suspensions measured by the rheometer and the evaluation of process performance will be studied in depth. It is to be investigated if the rheological properties can be controlled by adding particles for the variation of rheological properties. If so, a procedure can be proposed for the a systematic process stabilization method as shown in the Figure 1.5.

[8] Standard Of Procedure

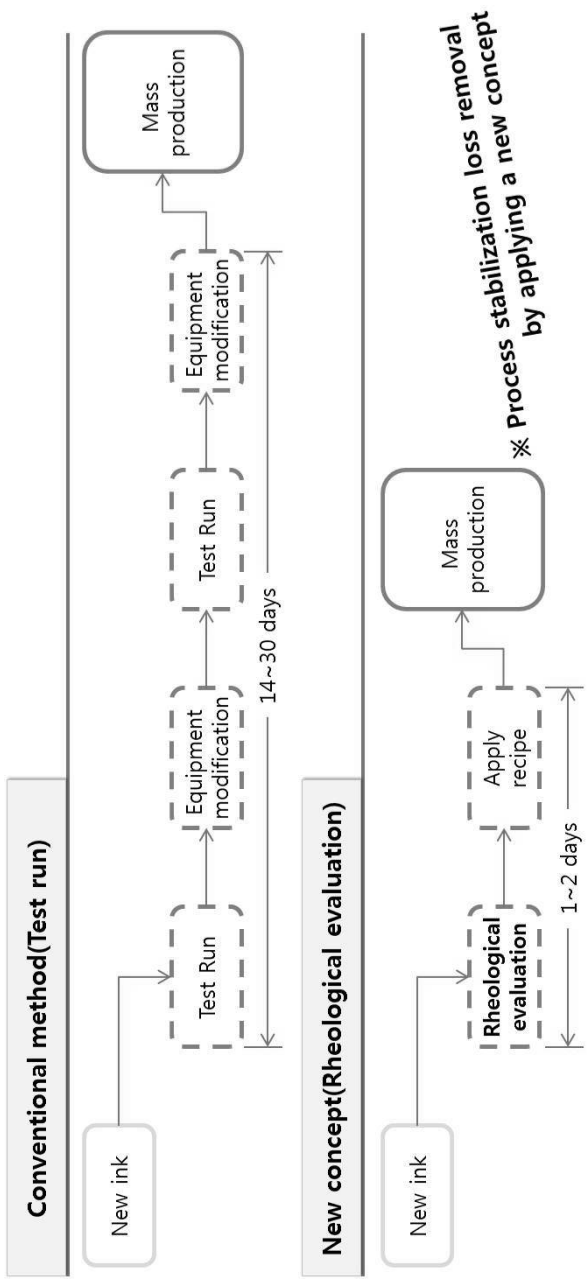

Figure 1.5: Systematic inkjet process stabilization improvement plan applying rheological property evaluation

1.3 Outline of the thesis

To improve the overall understanding of this paper and to easily find the necessary contents, we have arranged the overall contents as follows.

In Chapter 1, the background and purpose of the research are summarized. We explained the flow of technological development in the recently display industry and the necessity of introducing alternative technology, we proposed how this study could improve.

In Chapter 2, we organized the theoretical background of the paper and related to this study. Previous studies on inkjet Z numbers, capillary numbers for paints, and suspensions containing particles were summarized.

In Chapter 3, test results are discussed. The actual research on the change of rheological properties using suspension is described in detail.

Finally, Chapter 4 concludes by explaining the actual application plan of the research described in this work and the direction of future research is suggested.

Chapter 2

Related works

2.1 Rheology in Inkjet printing

The technology of inkjet printing has been developed in several ways since the past. Among them, the DOD[1] inkjet printing method was recognized as the most attractive manufacturing method due to its simplicity, cost efficiency, and versatility. Recently, using inkjet printing technology, thin-film transistors[1], displays using polymers[2], and products made by evaporating materials[3][4] are being manufactured. These applications have been greatly promoted through the development of new printable functional materials such as nano-particles, polymer semiconductors, OLED displays, etc. Unfortunately, research on material synthesis has developed dramatically through material development, but methods for operating printing devices are rare.

DOD inkjet printing technology is largely composed of TD[2] and PD[3] technology [5]. The TD type is composed of a small chamber including a heater in the printing head and is a method of injecting ink onto paper or substrate by increasing the pressure by heating the heater to create bubbles in the ink. The TD printing method does not require special equipment, so the equipment price is cheap, but it is difficult to operate precisely. The driving method used in most commercial and industrial applications is PD type. In the PD type, a piezoelectric element is installed instead of

[1] Drop On Demand
[2] Thermal Drop on demand
[3] Piezo electric Drop on demand

a heater to adjust the voltage waveform to increase the ink pressure to generate ink droplets. The PD type does not have unstable conditions such as bubble generation using heat, so it can use a variety of inks than the TD type and allows precise electrical manipulation. However, the use of piezoelectric elements has a disadvantage that the equipment price is more expensive.

With the development of inkjet printing in this way, studies that the rheological properties of ink react very sensitively to printing have been continuously conducted since the past. Inks with poorly designed rheological properties or operations that do not reflect rheological analysis can cause problems such as clogged nozzles or failure to reach the desired location. Due to the rheological effect, the contact angle of the ink droplet and the interaction of the other droplets on the substrate greatly affect the overall pattern shape[6][7], and the coffee ring effect that occurs during drying also impairs inkjet pattern uniformity[8][9]. For the above reasons, many researchers have argued that rheological analysis should be essential when using inkjet printing[10][11][12][13][14].

2.1.1 Z number

For successful inkjet printing, it must be well designed rheologically for ink droplet spray-ability and uniform deposition as well as the printed structure after drying. In particular, it is known that the spraying of a suspension differs from the Newtonian fluid in terms of a straight orbit, etc [15]. Poor spray-ability may cause difficulties and irregularities in the printing process and may cause a coffee ring effect caused by a concentration gradient and particle adsorption to the liquid-air interface in terms of diffusion and leveling. It is a very important study to characterize and analyze spraying phenomena to solve problems arising from the complexity of the ink composition itself as well as the printing process including such irregularities. Many factors affect the performance of inkjet printing. Fluid properties such as surface tension(σ), viscosity(η), and density(ρ) as well as processing parameters such as drive voltage, dwell time, and repetition rate is included. In the case of a Newtonian fluid, the drop formation is determined by the Z number (2.1), which is a dimensionless number, where d is the nozzle diameter, which is the characteristic length scale of the print head[16].

$$Z = (d\rho\sigma^{\frac{1}{2}})/\eta \tag{2.1}$$

The Z number is the reciprocal of the Ohnesorge number and can be expressed as Reynolds (Re) and Weber (We) numbers (2.2). If Z is too low, droplets cannot be formed, and if Z is too high, fine droplets are formed, resulting in poor printing quality. Tai et al. observed printing ejection using an aqueous mixture (0$\sim$80wt%) of various glycerol compositions in the range of $0.67 < Z < 50$. This shows that if the rheological parameters are considered in inkjet printing, printing quality can be

improved by adding a small amount of polymer to adjust the Z number[17].

$$Z = Oh^{-1} = Re/We^{\frac{1}{2}} \tag{2.2}$$

The Ohnesorge number(Oh) is an undimensioned number that relates viscous forces to inertia and surface tension, which was defined in 1936 by Wolfgang von Ohnesorge in his doctoral dissertation(2.3).

$$Oh = \frac{\mu}{\sqrt{\rho\sigma L}} \sim \frac{viscous forces}{\sqrt{inertia \bullet surface tension}} \tag{2.3}$$

Where μ is the dynamic viscosity of the liquid, ρ is the density of the liquid, σ is the surface tension, and L is the characteristic length (nozzle diameter). The Ohnesorge of raindrops with a diameter of 3 mm is generally 0.002 or less, and a larger Ohnesorge number means that the viscosity is more affected. In inkjet printing, liquids with an Ohnesorge number less than 1 and greater than 0.1 can be jetted. Converting to Z number means that printing is possible only when the Z number is greater than 1 and less than 10[6][18].

2.2 Contact angle and Capillary number

Research on the parameter controlling the contact angle has been ongoing since the past. Research has been divided into two major categories, relationship study using theoretical model[19][20][21][22][23][24] and a study through experiment[25] [26][27]. All of them defined that the control parameter of the contact angle was composed of the capillary number (Ca) as shown in the Equation (2.4).

$$\theta = f(Ca) \tag{2.4}$$

The capillary number (Ca) of the Equation (2.4) is a dimensionless number representing the relative effect of viscous drag and surface tension acting across the interface between a liquid and a gas or between two liquids(2.5)[28].

$$Ca = \frac{\mu V}{\sigma} \tag{2.5}$$

Where μ is the dynamic viscosity of the liquid, V is the characteristic velocity, and σ is the surface tension or interfacial tension between the two fluids. The number of capillaries plays an important role in the flow of capillaries, and in particular, it determines the dynamic contact angle of the liquid flowing at the interface[29].

Looking at the representative theories and experiments mentioned earlier, Bracke et al. used glycerol solution to control the contact angle by the velocity (V) of the number of capillaries, and as a result of the study, the relationship was defined as shown in the Equation (2.6) and the Figure 2.6[25].

$$cos\theta_d = cos\theta_0 - \gamma Ca^{\frac{1}{2}} \tag{2.6}$$

RICHARD L. HOFFMAN observed the increase and decrease of the contact angle according to the change of the number of capillaries and the transfer coefficient using silicone type Admex 760 and Santicizer 405 liquid in 1975. As a result, it was said that the two are closely connected as shown in the Figure 2.7[30]. Besides, GORAN STROM et al. studied another type of experimentation of contact angle. In 1987, it was an experiment to find out how the contact angle of silicone oil changes on flat and capillary surfaces made of glass and polystyrene. As a result of the study, it was explained that it is connected to the number of capillaries as shown in the Figure 2.8[23].

As such, the relationship between the contact angle and the capillary number has been studied until now through experiment [31],[32], and simulation [33]. In this paper, we will also study the correlation between the contact angle and the number of capillaries through an experiment of slide coating a paint that is widely used commercially.

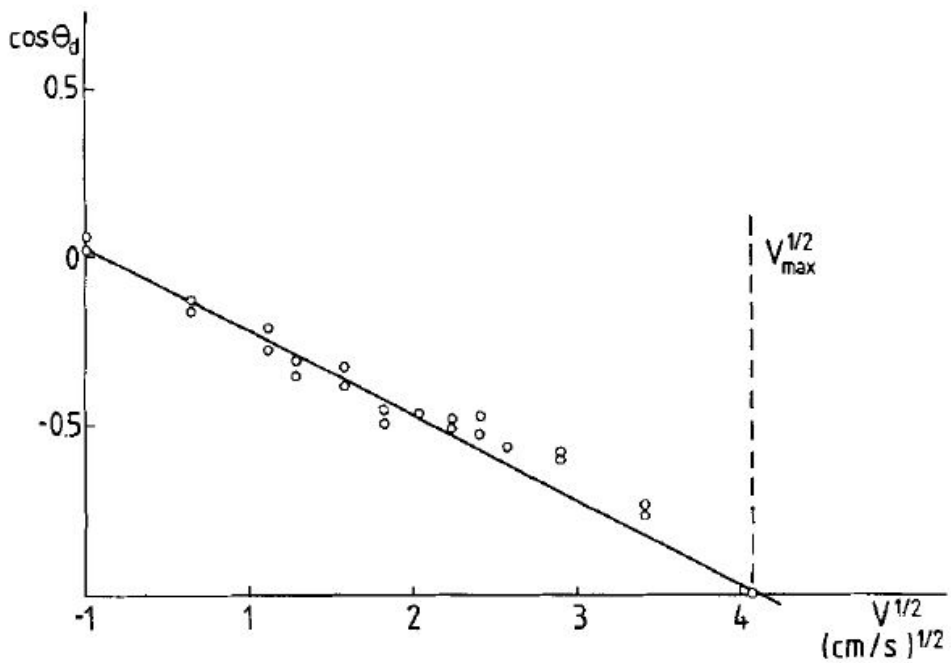

Figure 2.6: Smooth polyethylene strip was drawn into an aqueous glycerol solution

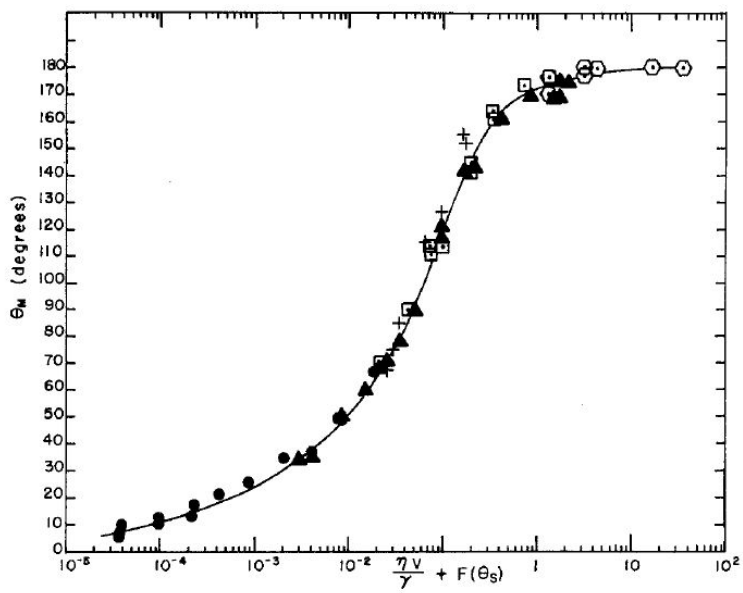

FIG. 5. Effect of flow on the apparent contact angle of an advancing liquid–air interface: (●) G.E. Silicone SF-96, $F(\theta_s) = 0$; (▲) Brookfield Silicone, $F(\theta_s) = 0$; (⊙) Dow Corning Silicone, $F(\theta_s) = 1.5 \times 10^{-4}$; (⊡) Ashland Chemical Admex 760, $F(\theta_s) = 2.35 \times 10^{-2}$; (+) Santicizer 405, $F(\theta_s) = 2.1 \times 10^{-2}$; the data were taken at 24°C.

Figure 2.7: Effect of flow on the apparent contact angle of an advancing liquid-air interface

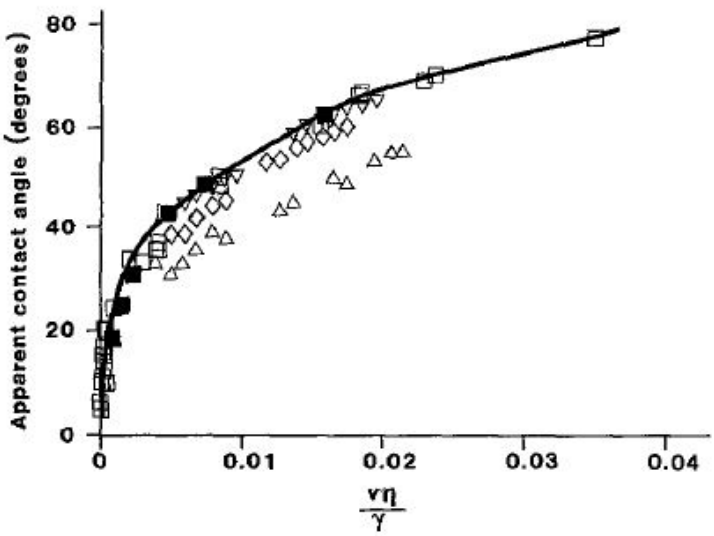

FIG. 4. Apparent dynamic contact angles obtained for liquids spreading in different geometries. Silicone oil spreading between plane and parallel glass surfaces of nominal separation 0.1 mm (△), 0.7 mm (◇), and 1.2 mm (▽) (29). Silicone oil spreading in a capillary tube with a diameter of 2.0 mm (□) (1). Silicon oil spreading against a single plane polystyrene surface (■) (this work).

Figure 2.8: Apparent dynamic contact angles obtained for liquids spreading in different geometries

2.3 Volume fraction in Suspension Rheology

Albert Einstein attempted to deduce the relationship between the size of a molecule and the viscosity of a solution in his doctoral thesis[34]. He derives the relationship between the volume fraction and viscosity, assuming that the molecule is a hard-sphere(particle) (2.7).

$$\eta = \eta_m(1+\phi) \tag{2.7}$$

But a few years later, Jean Perrin measured the viscosity of the suspension in the lab, which was much higher than Einstein's predictions. In response, Einstein found an error in the differentiation of the velocity component and published an accurate result by referring to Perrin's experiment in 1911[35]. Einstein's viscosity equation, created in this way, not only estimates the hydrodynamic volume of molecules in solution but also is still used in suspension rheology (2.8).

$$\eta = \eta_m(1+2.5\phi) \tag{2.8}$$

To explain the relationship between particle volume fraction and viscosity, many researchers besides Einstein have proposed empirical equations. Zarraga et al. proposed a relational expression (2.9) suitable for ϕ_{max}=0.62 in his paper [36].

$$\eta_r(\phi) = e^{-2.34\phi}\left(1-\frac{\phi}{\phi_{max}}\right)^{-3} \tag{2.9}$$

At the same time, the Eilers Equation (2.10) was also published, which was

suitable for the data case with a volume ratio of ϕ_{max}=0.58.

$$\eta_r = \left[1 + 1.5\phi\left(1 - \frac{\phi}{\phi_{max}}\right)^{-1}\right]^2 \tag{2.10}$$

In this way, the Equations (2.9)(2.10) can fit the viscosity curve according to each maximum volume ratio, but it was impossible to accurately deduce the viscosity of other maximum volume ratios from the equations. As shown in the Figure 2.9, it can be seen that the value and shape of the graph are greatly different according to the change of the maximum volume ratio[37].

For the above reasons, two equations are selectively used in general applications of suspension rheology. The first Equation (2.11) was proposed by Krieger and Dougherty[38]. In the equation, η_r is the effective viscosity, ϕ is the volume fraction, ϕ_{max} is the maximum volume fraction, and ρ is the density.

$$\eta_r = \left(1 - \frac{\phi}{\phi_{max}}\right)^{-[\eta]\rho\phi_{max}} \tag{2.11}$$

The second Equation (2.12) is a special form of the Maron-Pierce equation [39] popularized by Quemada.

$$\eta_r = \left(1 - \frac{\phi}{\phi_{max}}\right)^{-2} \tag{2.12}$$

Using the Equations (2.11)(2.12), the viscosity of a suspension to which spherical particles are added can be completely predicted given only the basic viscosity, particle volume fraction, and maximum volume fraction.

In this paper, as an experiment using silicone oil and PMMA spherical particles, the relationship between the volume fraction and rheological properties of particles is studied and compared with previous studies.

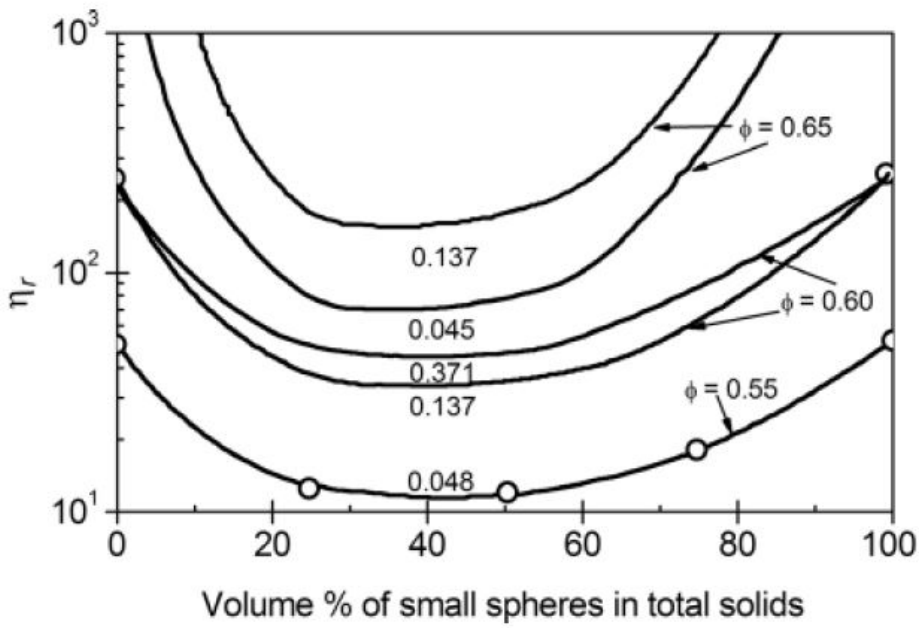

Figure 2.9: Effect of the particle size distribution on the relative viscosity for bimodal suspensions

Chapter 3

Experimental methods and Results

3.1 Controlling Contact angle of Paints

The purpose of this experiment is to study the relationship between the coating process result(contact angle). The commercial paint and the number of capillaries were researched to get whether the process result can be predicted in advance by analyzing the rheological properties.

3.1.1 Equipment and Sample preparation

As experiment material, 5 colors of Samwha's DIY pastel paint were used. Colors were randomly selected as white, yellow, green, sky blue, and orange. It was assumed that these paints behave similar as ink. Three experimental equipment were used for the evaluation of paint rheological properties and the comparison of results. First, for the production of experimental samples, Zehntner's ZAA-2300 coater was modified to allow line coating as shown in the Figure 3.11 with a jig made by 3D printer. Initially, jigs were manufactured in Point type, Line type, and Open type as shown in the Figure 3.10. However, since the paint is more viscous than actual ink and contains a large number of particles, clogging occurs frequently in the point type and line type during the experiment. So the experiment was conducted using an open type jig. The open type jig was fixed at 30 degrees in this experiment, but the changing angle was not tried. 10 samples were produced for each color as shown in the Figure

3.12 using the modified equipment. For the analysis of the rheological properties of the paint, an AR-G2 rheometer of TA company was used with a 40mm flat plate for the measurement module. And the pre-shear 500 s^{-1} was maintained for 30 seconds for all the experiments. After that, the viscosity value in the range of 0.1$\sim$100 s^{-1} of shear rate was measured. Finally, to measure the lateral contact angle, which is the result of the process, the height difference of the Figure 3.13 was analyzed to obtain the data in a FOV[1] range of 2.5 x 2.5 mm at 2 µm per height step in precision mode using an Olympus OLS3000 confocal microscope.

Figure 3.10: Jigs produced by 3D printer (point, line, open type from left)

[1]Field Of View

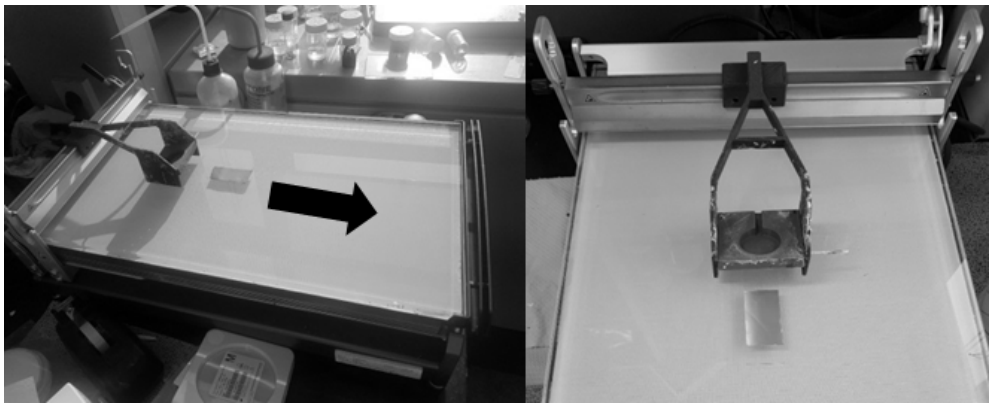

Figure 3.11: Slide coater (ZAA-2300)

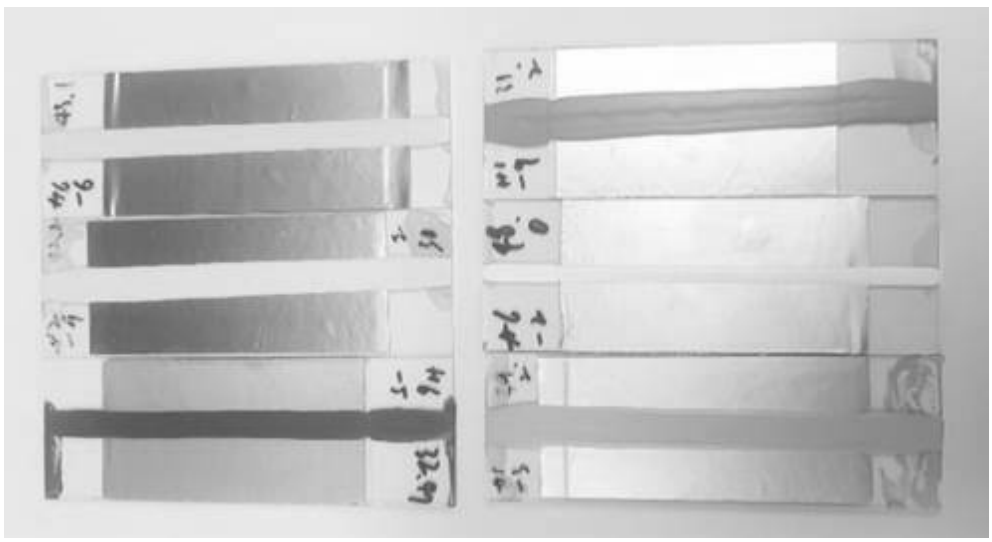

Figure 3.12: Produced samples

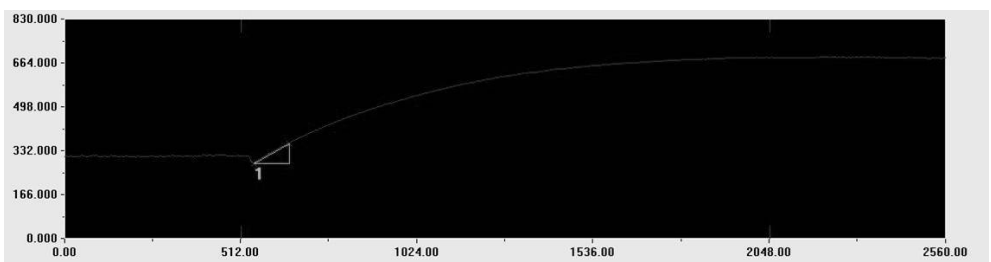

Figure 3.13: Data measured height using an confocal microscope

3.1.2 Height measurement of contact angle

Samples were made by the slide coater, the contact angles were manually measured with a deviation of +/- 5° as shown in the Figure 3.14 and the average value of the contact angle was shown in the Figure 3.15. The contact angle for each paint color, samples measured every 1∼5°, and the values decrease in the order of white, yellow, sky blue, green, and orange. The highest value of the contact angle is 45.43° in white and the lowest value is 31.06° in orange. The points that do not converge horizontally is considered to be the limit of the measurement area of the microscope, and if the FOV is widened, all the data are expected to converge horizontally.

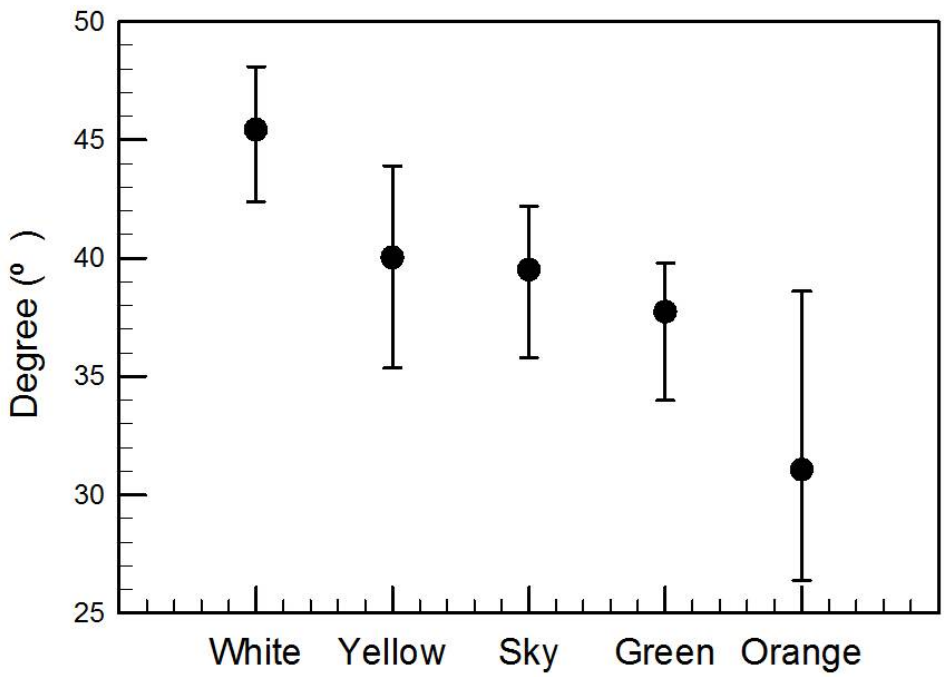

Figure 3.14: Data range of measured contact angles

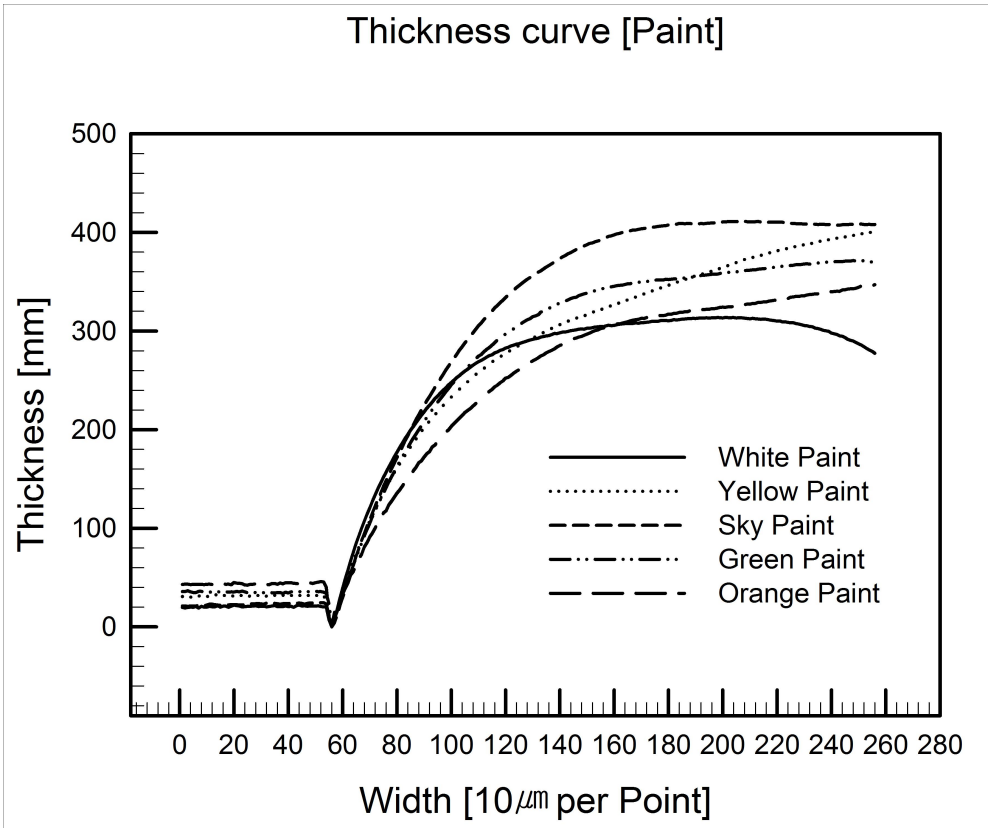

Figure 3.15: The results of measuring the contact angle of paints.

3.1.3 Rheological analysis of contact angle

The viscosity was measured using AR-G2 without a reversal in the range of $0.1 \sim 100 s^{-1}$ shear rate. The viscosity is distributed within 0.42∼27.7 Pa.s as shown in the Figure 3.16, and it was shown that the viscosity decreases in the order of white, yellow, sky blue, green, and orange. At shear rate of $10^0 s^{-1}$, which is the predicted shear rate value of the actual line coating, the viscosity values are summarized in the Table 3.2 in the next section.

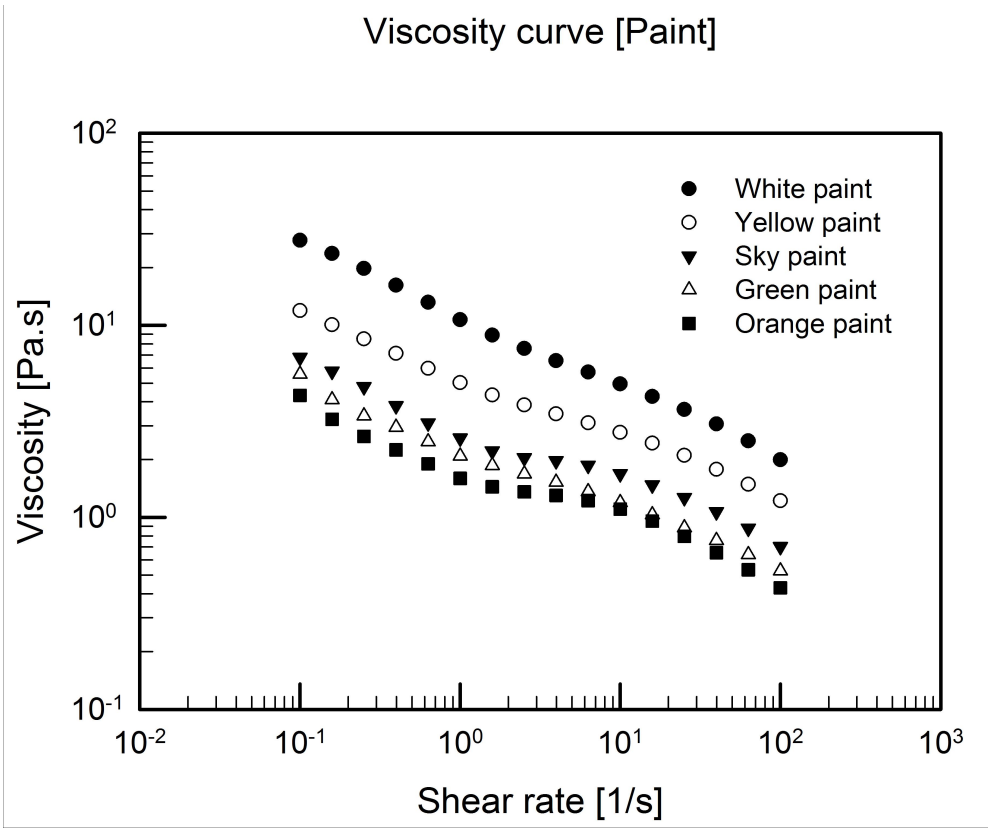

Figure 3.16: Viscosity values by paints

3.1.4 Tendency of contact angle and viscosity

There shows a certain tendency between contact angle and viscosity. As contact angle decreases, the viscosity decreases as shown in the Table 3.2. And additional experiments are required to predict the absolute value of the contact angle. Since this experiment focused on μ (viscosity value) among the variable of capillary number, a further study is necessary to measure σ (surface tension) with a tensiometer and to seeing the contact angle could be predicted.

Table 3.2: Comparison of contact angle and viscosity values

Colors	Contact angle(°)	Viscosity(Pa.s)
White	45.43	10.70
Yellow	40.13	5.03
Sky	39.51	2.59
Green	37.74	2.08
Orange	31.06	1.60

3.2 Effect of particles on Silicone oil

This experiment was conducted to see whether the viscosity can be controlled by adding micro-sized particles.

3.2.1 Suspension preparation

The silicone oil/PMMA sample made by Dr. Ju-Yong Moon was used to study the change in rheological properties according to the particle size and content of the suspension[40]. Silicone oil is a liquid polymerized siloxane (Si-O-Si) with organic side chains. Its main composition is polydimethylsiloxane. It is an oily liquid that does not have taste and smell and is widely used commercially due to its high thermal stability and lubrication properties. KF-96 100cs(Shinetsu, Inc., Japan) was used as a standard silicone oil. The e-VROC can measure the viscosity in the range of 1.0∼2000mPa.s, and the accuracy is guaranteed to be within +/- 2%. Detailed technical specifications are summarized in the Table 3.3. The model solution for this experiment is spherical mono-disperse poly(methyl methacrylate)(PMMA) particles dispersed in silicone oil.

Table 3.3: e-VROC technical specifications

Technical specifications	
Minimum Sample	500 $\mu\ell$
Viscosity Range	1.0-2000 mPa.s
Shear Rate Range	0.1-1000 s^{-1}
Accuracy	+/-2 %
Flow channel	50, 100μm

The density of the model solution matched relatively well at 965 and 1180 kg/m^3, so that particle sedimentation during the experiment could be neglected.

Three types of PMMA particles (1 µm, 5 µm, a 1:1 ratio 1 µm and 5 µm) were used as the suspension. The particles were added to the silicone oil as specified in the Table 3.4 and then stirred for 30 minutes using an ultrasonic disperser VCX-750(Sonics materials, Inc.). After the dispersion was completed, the suspension was further mixed in a magnetic stirrer MS-MP8(DAIHAN Scientific, inc.) for maintaining better dispersed status.

Table 3.4: Content of silicone oil and PMMA according to a volume fraction

PMMA Volume fraction	Si-Oil(g)	PMMA(g)
2%	63.05	1.57
5%	61.12	3.93
10%	57.90	7.87
15%	54.68	11.80

To check the degree of the suspension, an optical microscope was used and it was confirmed that all three types of suspension were as shown in the Figure 3.17, 3.18, 3.19.

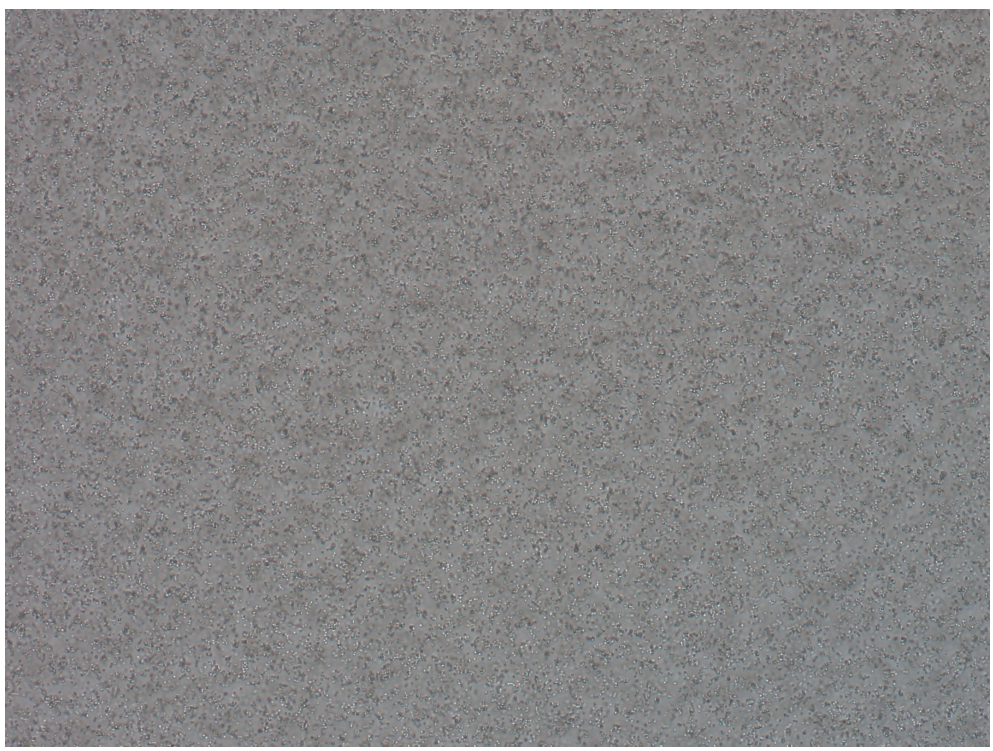

Figure 3.17: Image of the suspension containing 1μm particle at 20x

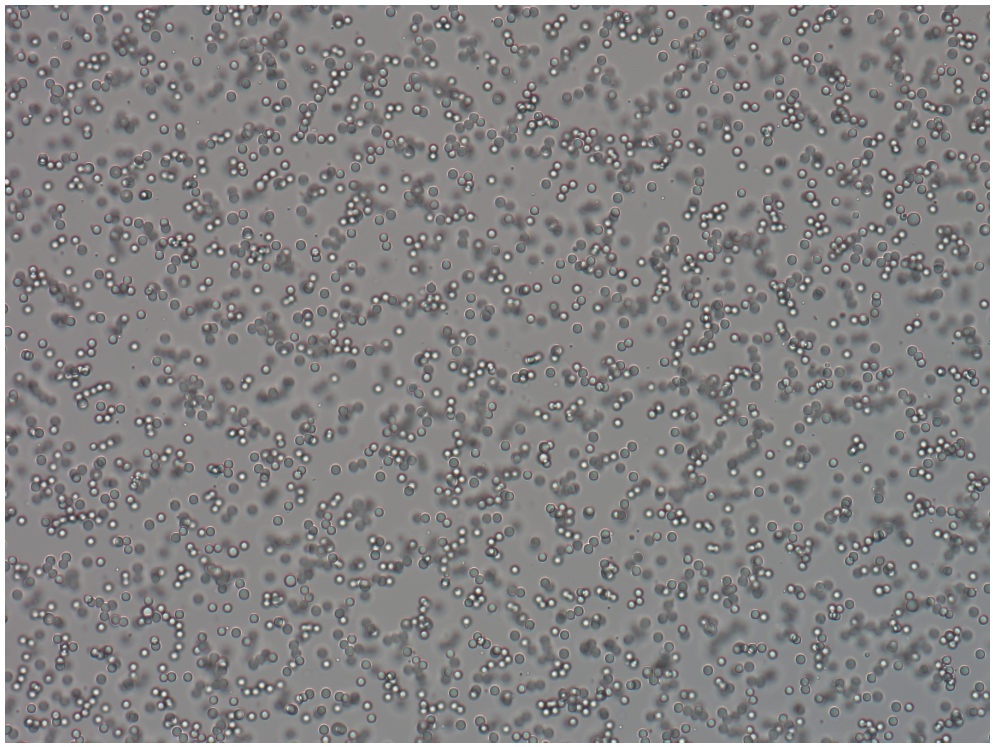

Figure 3.18: Image of the suspension containing 5μm particle at 20x

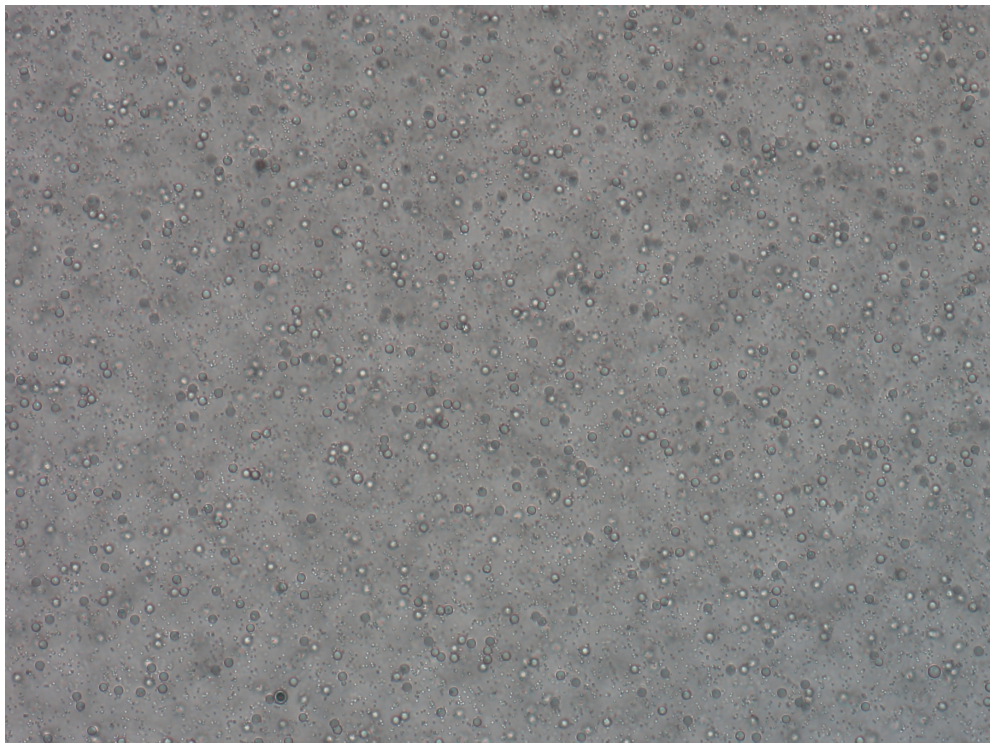

Figure 3.19: Image of suspension containing 1μm and 5μm particle at 20x

3.2.2 Rheological properties analysis

To measure the viscosity of the suspension, the e-VROC B10 chip was used for the range of the shear rate between 299 and 1498 s^{-1}, and the E05 chip was used for the range of the shear rate between 1548 and 19365 s^{-1}. The B10 chip has a 100μm flow channel. So there was no channel blockage during measurement in the case of 5μm and 1μm PMMA particles. But in the measurement using an E05 chip with a channel height of 50 μm, clogging of the channels occurred frequently. Hence the viscosity of 5 μm particles could be obtained only. It was shown that the ranges of the two chips were well connected as shown in the Figure 3.20. If the channel clogging problem was resolved, it would be possible to analyze the rheological properties in the high shear rate area of various particle size suspensions.

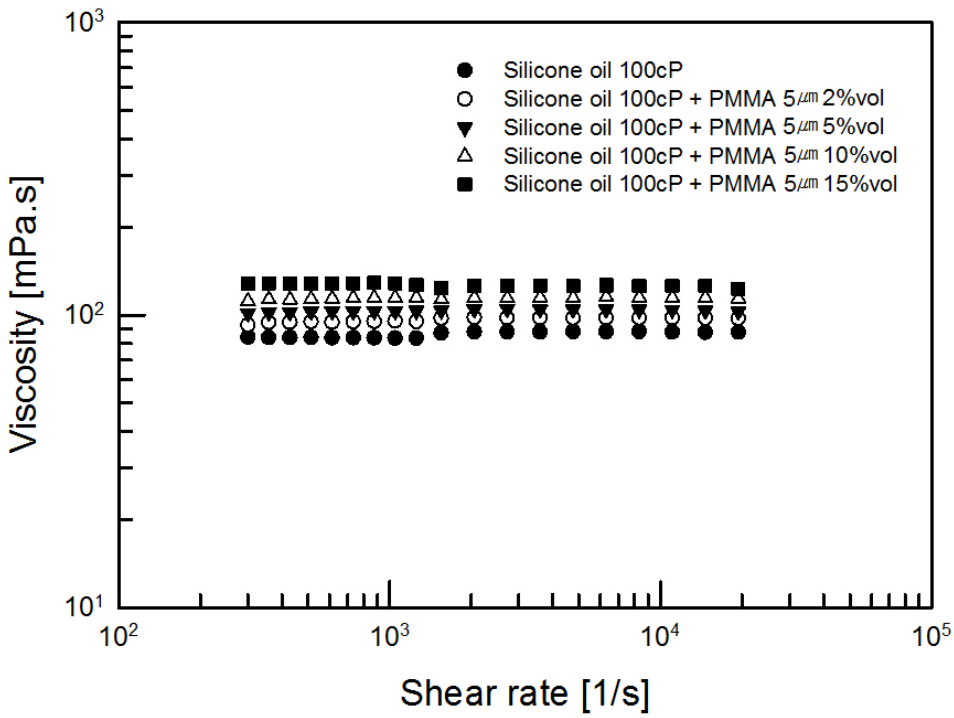

Figure 3.20: The results of connecting data of B10, E05 chips (PMMA 5㎛)

The Krieger and Dougherty equation defined in the Equation (3.1) was used to evaluate the reliability of the measured data[41]. When the medium viscosity (η) of the suspension is below 84mPa.s and the maximum volume ratio is defined as ϕ_{max} = 0.64, the measured effective viscosity was well matched with the calculated effective viscosity as shown in the Figure 3.21.

$$\eta_r = \left(1 - \frac{\phi}{\phi_{max}}\right)^{-[\eta]\rho\phi_{max}} \tag{3.1}$$

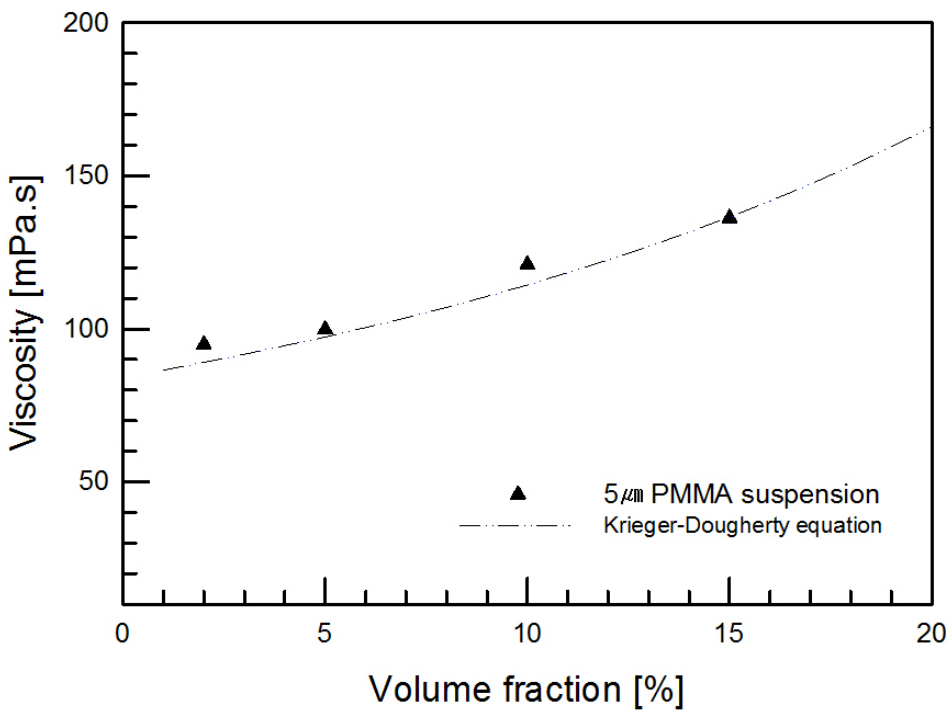

Figure 3.21: Effective viscosity of silicone oil / PMMA suspension(symbol) and calculated viscosity of the suspension using the Krieger-Dougherty equation as a function of the particle volume fraction(line)

In addition, the Einstein equation defined in the Equation (3.2) was used as well for the comparison[42][43]. The measured effective viscosity was also well matched with the calculated effective viscosity as shown in the Figure 3.22.

$$\eta = \eta_m(1+2.5\phi) \tag{3.2}$$

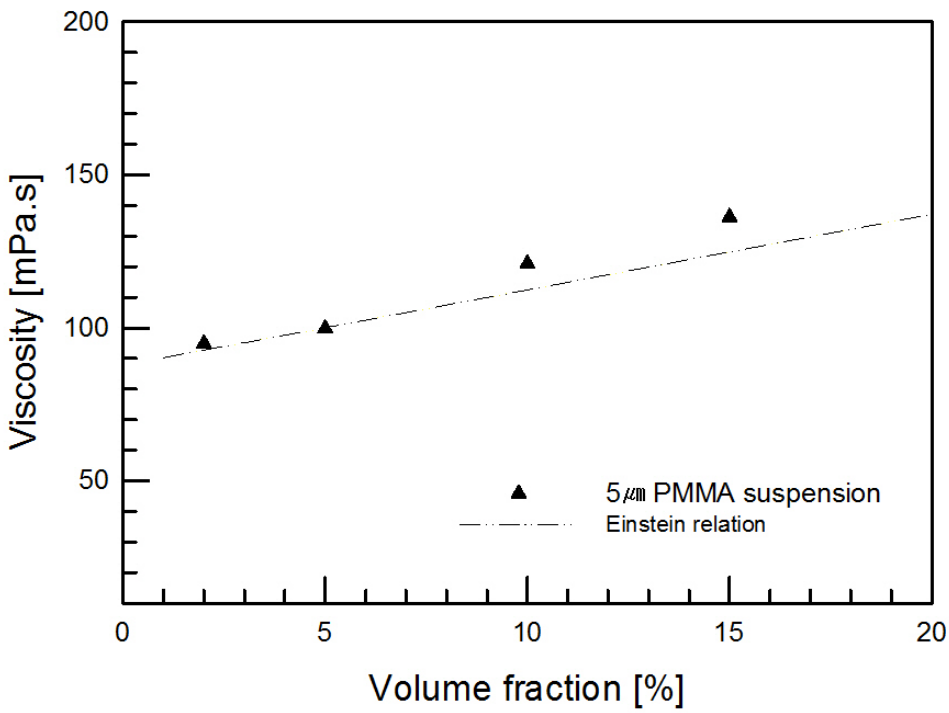

Figure 3.22: Effective viscosity of silicone oil / PMMA suspension(symbol) and calculated viscosity of the suspension using the Einstein equation as a function of the particle volume fraction(line)

With this results, the data measured by the experiment confirmed can be utilized for further analysis.

The data measured for dispersing 1㎛, 5㎛ PMMA particles in silicone oil at 2, 5, 10, 15 vol% contents are summarized in the Figure 3.23 and 3.24. And the data measured with mixing 1, and 5㎛ PMMA particles at the ratio of 1:1 and dispersing them in 2, 5, 10, and 15 vol% in silicone oil are shown in the Figure 3.25. It was confirmed that the measured data were well aligned with respect to the volume ratio.

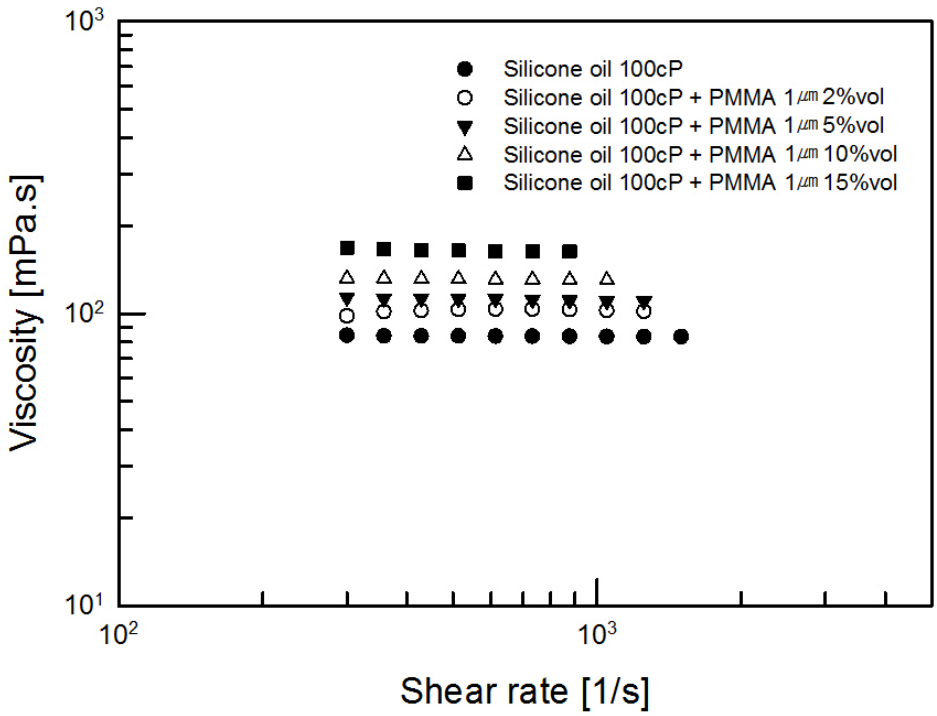

Figure 3.23: Measurement results by dispersing 1㎛ PMMA particles in silicone oil

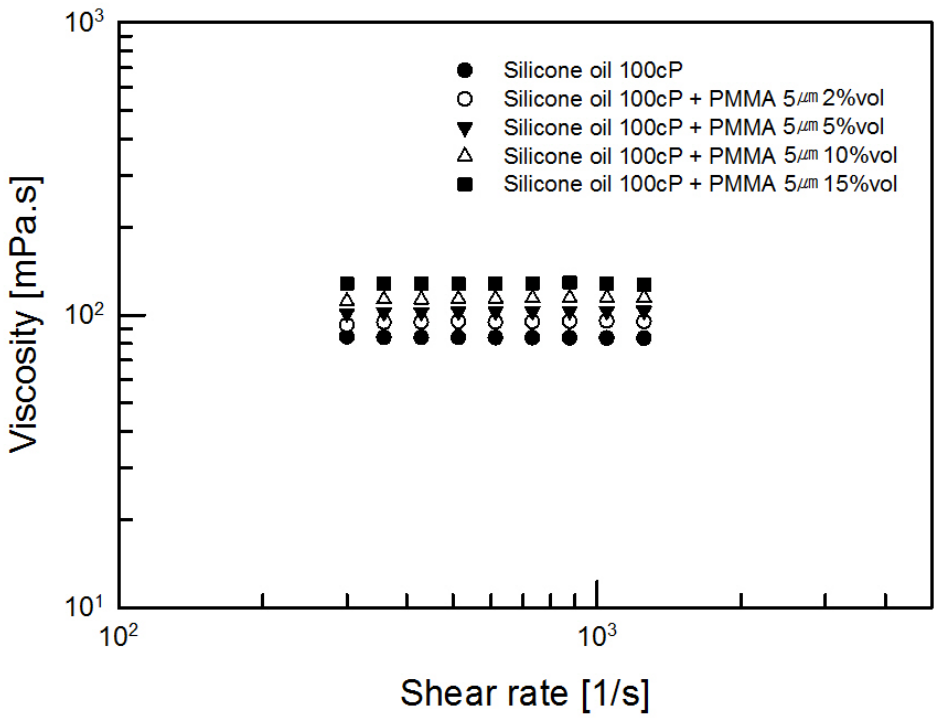

Figure 3.24: Measurement results by dispersing 5㎛ PMMA particles in silicone oil

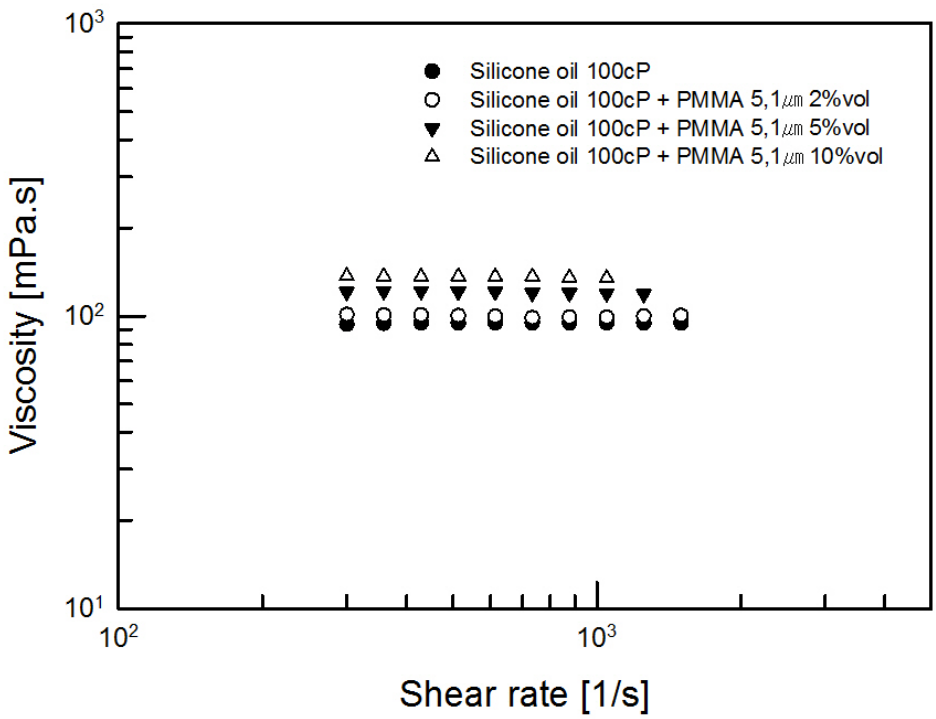

Figure 3.25: Measurement results by dispersing 1, 5㎛ PMMA particles in silicone oil at a ratio of 1:1

3.2.3 Controlling of viscosity by adding particles

With the experiments of adding PMMA particles, it was shown that when PMMA particles were added to silicone oil, the viscosity could be increased from 10% to 100% as shown in the Table 3.5. Figure 3.26 is a graph comparing 1㎛, 5㎛, 1&5㎛ (1:1 ratio mixing) PMMA particles at the shear rate $612s^{-1}$. When 1㎛ PMMA particles were added, it was confirmed that the viscosity changed the most, and there was a relatively small change in the case of 5㎛ particles. And the viscosity change of the suspension made by mixing 1㎛ and 5㎛ 1:1 was located between 1㎛ and 5㎛. This is a phenomenon that when the particle size is small, the contact area increases and the resistance increases. Looking at the change according to the volume ratio, the 5㎛ and 1&5㎛ suspensions had similar viscosity in the region below 10%. However, it was confirmed that the influence of the particle size appeared in earnest in the region of 10% or more.

Table 3.5: Viscosity difference according to PMMA particle size and volume

PMMA volume	PMMA 5㎛	PMMA 1&5㎛	PMMA 1㎛
0%	83.6770	83.6770	83.6770
2%	94.5890	94.8500	103.5390
5%	103.0170	99.8050	112.4350
10%	113.9480	121.0530	130.9520
15%	128.4270	136.1920	163.2540

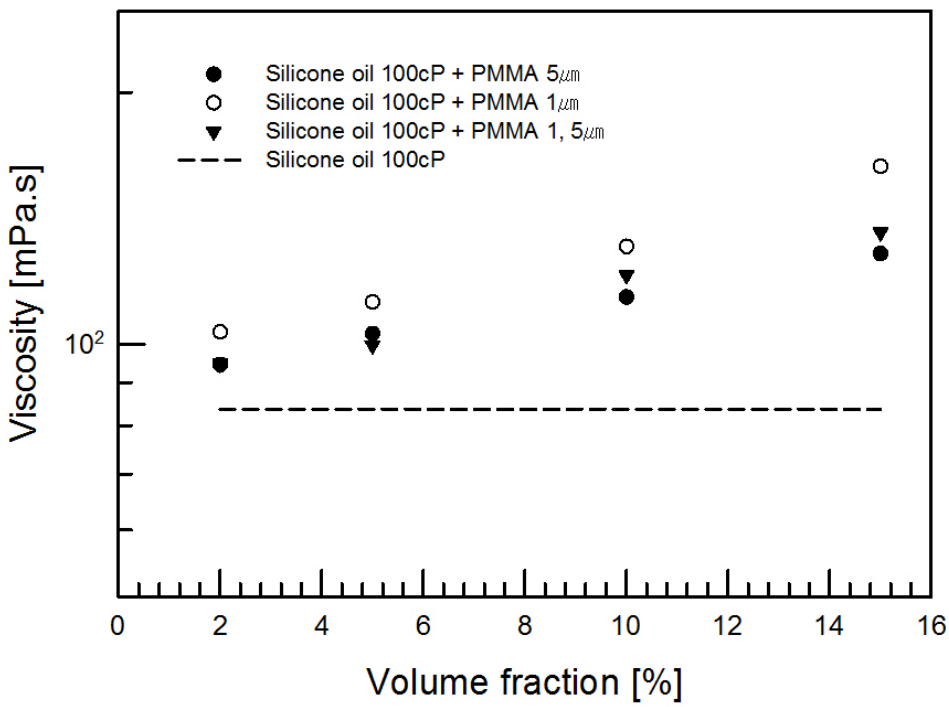

Figure 3.26: Viscosity difference according to PMMA particle size, volume at shear rate $612s^{-1}$

Chapter 4

Conclusion and Suggestion

In this study, it was investigated to see the possibility for setting up the standardized procedure of inkjet printing technology through the evaluation of rheological properties. As discussed in the Chapter 1, the operating condition of the equipment was set by the actual process performance. The results of this study can be a basis for further study to find the best solution for the standardized process. A protocol for the standardized procedure can be chosen by analyzing the rheological properties of a liquid.

The summary of the experimental results of this study is as follows.

First, it was shown that base on the tendency between viscosity and contact angle, it is possible to predict the contact angle by the interpolation, which is important parameter for the inkjet printing process. It was proved that the contact angle is increased with the viscosity increase.

Second, the rheological behavior was evaluated through the addition of PMMA particles to the silicone oil. It was found that the viscosity increases with the volume fraction of the particles increase. And it was found that the viscosity increases to 100% at the volume fraction of about 15 vol%.

Third, it was investigated the effect of particle size change on the rheological properties. It was found that the larger the particle, the less the change in rheological properties. And it was confirmed that the mixture of 1 µm and 5 µm at a 1:1 ratio, have mid-point rheological properties of 1 µm and 5 µm.

Based on the above three results, if the viscosity is measured and used as a reference value, the performance of the inkjet printing process can be predicted, and the rheological property can be controlled by adding particles to a specific liquid. And if this is applied to the display liquid-phase process, the equipment stabilization time can be significantly reduced.

The results of this study can be applied as follows.

Previously, in order to stabilize the equipment whenever there is a change in liquid, for adjusting and stabilizing the equipment, number of tests should be conducted. This was unavoidable because there was no standard procedure in case there are changes in liquid. Therefore, if the method of analyzing the rheological properties of liquids based on this study is applied, the existing commissioning method can be sufficiently improved, each time a material is changed, unnecessary test and process correction time can be reduced. In order to apply this study to the display liquid phase process, the work of linking the rheological property values, equipment adjustment history, and process results of the liquid materials used so far must be preceded. This is because stabilization must be based on previous data.

The proposed inkjet stabilization process through this study can be largely divided into 4 steps as shown in Figure 4.27.

First, the rheological properties of liquid materials used so far are evaluated, and equipment operation condition optimized for each liquid material are classified.

Second, select the rheological property to be referenced in the classified data.

Third, the reference rheological property of the new ink is measured.

Finally, stabilize the equipment by setting it according to the set recipe of the past ink, such as the same reference rheological property. If the ink does not have the same value, it can be equalized by adding particles.

We tried the above stabilization process using the Table 4.6 and 4.7. If the inks used so far have been evaluated and the setting recipe has been classified, and the rheological value of the new ink is the same as that of Ink B, it is possible to stabilize by setting the equipment according to the recipe of Ink B without a separate process test run. In the example, only five types of inks are expressed, but if the ink and recipes are summarized, the number of data will be more than thousands and more specific values can be obtained. Furthermore, if the data that connects the rheological characteristic value and the optimal recipe is accumulated in large quantities and converted into big data, the big data and machine learning part of the Figure 4.28 can be implemented. With this implementation, it is possible to develop an new process stabilization system that automatically analyzes rheological properties, adjusts the rheological properties and applies a specific recipe when new materials are introduced.

Table 4.6: Examples of ink rheological properties

Categories	Viscosity	Modulus(G‘)	Modulus(G“)
Ink A	Mid	High	Low
Ink B	Low	Mid	High
Ink C	Low	Low	Mid
Ink D	Low	High	Low
Ink E	High	Mid	High
New ink	Low	Mid	High

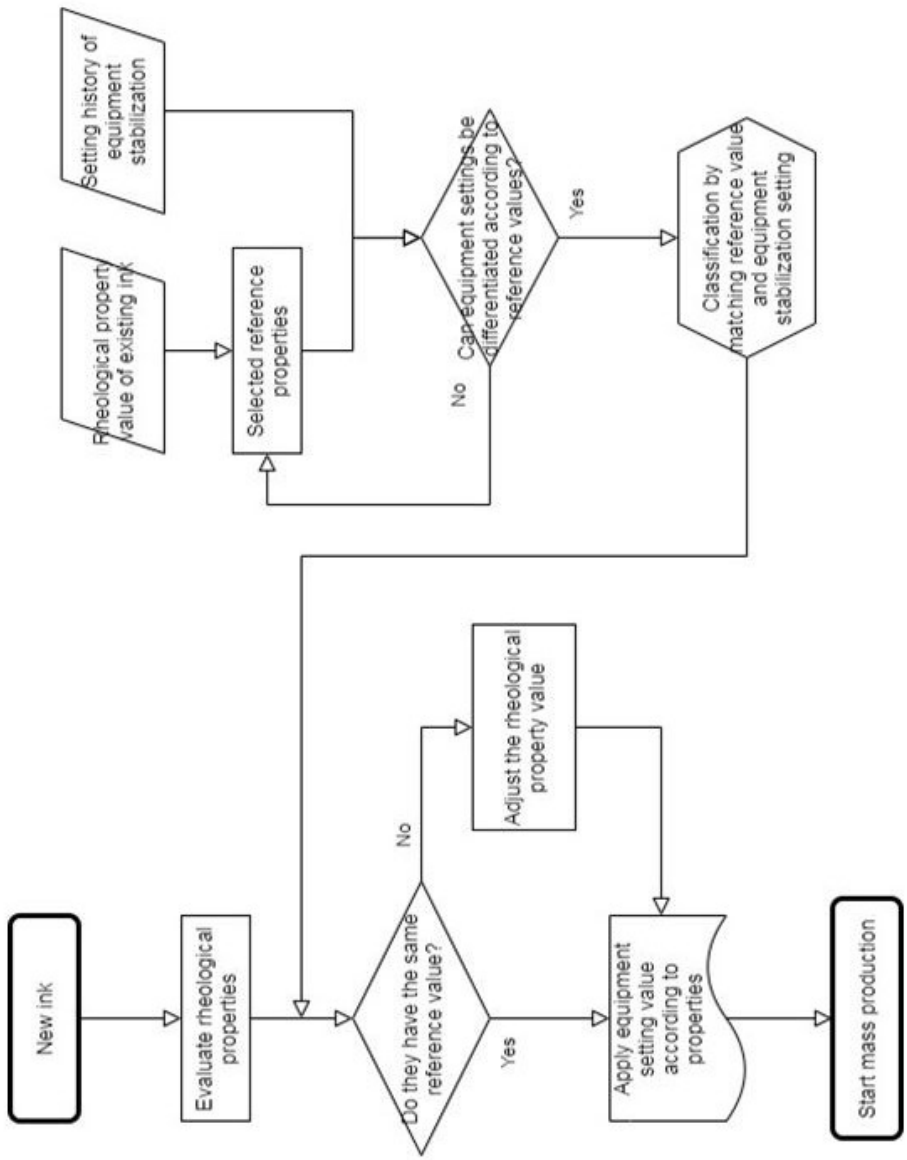

Figure 4.27: Flowchart of the inkjet stabilization process

Table 4.7: Examples of equipment stabilization settings

Categories	Head shape	Flow rate(mm/s)	Dispersion time(hr)	Duct type
Ink A	A type	10	1	A type
Ink B	B type	20	2	C type
Ink C	C type	25	3	B type
Ink D	A type	10	1	A type
Ink E	B type	25	2	E type

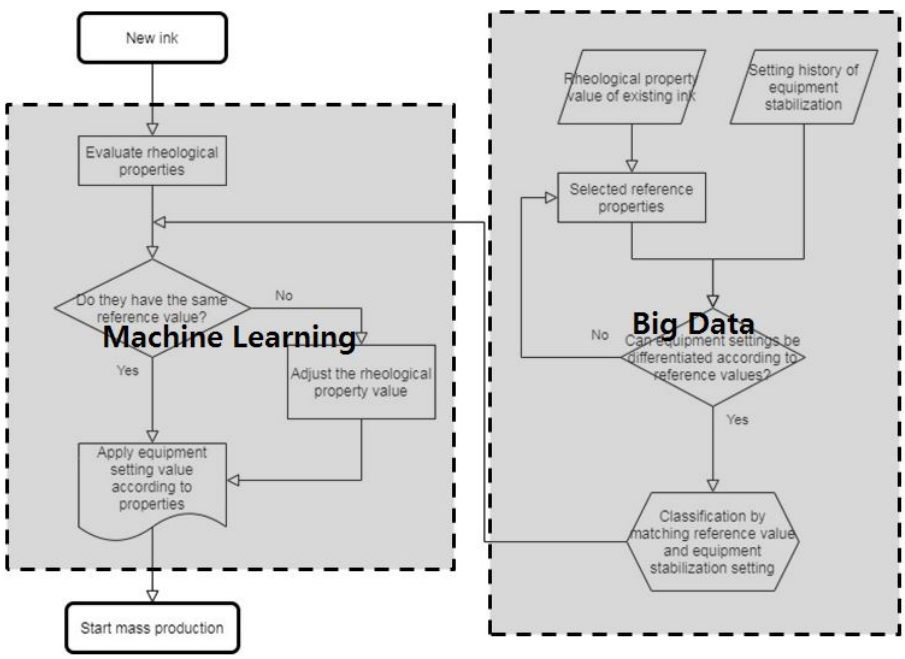

Figure 4.28: Unmanned inkjet stabilization method applying machine learning and big data

Bibliography

[1] H. Sirringhaus, T. Kawase, R. Friend, T. Shimoda, M. Inbasekaran, W. Wu, and E. Woo, "High-resolution inkjet printing of all-polymer transistor circuits," *Science*, vol. 290, no. 5499, pp. 2123–2126, 2000.

[2] J. Bharathan and Y. Yang, "Polymer electroluminescent devices processed by inkjet printing: I. polymer light-emitting logo," *Applied Physics Letters*, vol. 72, no. 21, pp. 2660–2662, 1998.

[3] A. Atkinson, J. Doorbar, A. Hudd, D. Segal, and P. White, "Continuous ink-jet printing using sol-gel "ceramic" inks," *Journal of Sol-Gel Science and Technology*, vol. 8, no. 1-3, pp. 1093–1097, 1997.

[4] R. Danzebrink and M. A. Aegerter, "Deposition of micropatterned coating using an ink-jet technique," *Thin Solid Films*, vol. 351, no. 1-2, pp. 115–118, 1999.

[5] H. P. Le, "Progress and trends in ink-jet printing technology," *Journal of Imaging Science and Technology*, vol. 42, no. 1, pp. 49–62, 1998.

[6] B. Derby, "Inkjet printing of functional and structural materials: fluid property requirements, feature stability, and resolution," *Annual Review of Materials Research*, vol. 40, pp. 395–414, 2010.

[7] D. Soltman and V. Subramanian, "Inkjet-printed line morphologies and temperature control of the coffee ring effect," *Langmuir*, vol. 24, no. 5, pp. 2224–2231, 2008.

[8] R. D. Deegan, O. Bakajin, T. F. Dupont, G. Huber, S. R. Nagel, and T. A. Witten, "Capillary flow as the cause of ring stains from dried liquid drops," *Nature*, vol. 389, no. 6653, pp. 827–829, 1997.

[9] R. D. Deegan, "Pattern formation in drying drops," *Physical review E*, vol. 61, no. 1, p. 475, 2000.

[10] K. A. Seerden, N. Reis, J. R. Evans, P. S. Grant, J. W. Halloran, and B. Derby, "Ink-jet printing of wax-based alumina suspensions," *Journal of the American Ceramic Society*, vol. 84, no. 11, pp. 2514–2520, 2001.

[11] B. Derby and N. Reis, "Inkjet printing of highly loaded particulate suspensions," *MRS bulletin*, vol. 28, no. 11, pp. 815–818, 2003.

[12] N. Reis, C. Ainsley, and B. Derby, "Viscosity and acoustic behavior of ceramic suspensions optimized for phase-change ink-jet printing," *Journal of the American Ceramic Society*, vol. 88, no. 4, pp. 802–808, 2005.

[13] C. Ainsley, N. Reis, and B. Derby, "Freeform fabrication by controlled droplet deposition of powder filled melts," *Journal of materials science*, vol. 37, no. 15, pp. 3155–3161, 2002.

[14] P. Calvert, "Inkjet printing for materials and devices," *Chemistry of materials*, vol. 13, no. 10, pp. 3299–3305, 2001.

[15] X. Wang, W. W. Carr, D. G. Bucknall, and J. F. Morris, "Drop-on-demand drop formation of colloidal suspensions," *International journal of multiphase flow*, vol. 38, no. 1, pp. 17–26, 2012.

[16] A. Lee, K. Sudau, K. H. Ahn, S. J. Lee, and N. Willenbacher, "Optimization of experimental parameters to suppress nozzle clogging in inkjet printing," *Industrial & engineering chemistry research*, vol. 51, no. 40, pp. 13195–13204, 2012.

[17] J. Tai, H. Y. Gan, Y. N. Liang, and B. K. Lok, "Control of droplet formation in inkjet printing using ohnesorge number category: materials and processes," in *2008 10th Electronics Packaging Technology Conference*, pp. 761–766, IEEE, 2008.

[18] G. H. McKinley and M. Renardy, "Wolfgang von ohnesorge," *Physics of Fluids*, vol. 23, no. 12, p. 127101, 2011.

[19] R. L. Hoffman, "A study of the advancing interface: Ii. theoretical prediction of the dynamic contact angle in liquid-gas systems," *Journal of Colloid and Interface Science*, vol. 94, no. 2, pp. 470–486, 1983.

[20] L. Tanner, "The spreading of silicone oil drops on horizontal surfaces," *Journal of Physics D: Applied Physics*, vol. 12, no. 9, p. 1473, 1979.

[21] R. Cox, "The dynamics of the spreading of liquids on a solid surface. part 1. viscous flow," *Journal of Fluid Mechanics*, vol. 168, pp. 169–194, 1986.

[22] T. Blake, "Wetting kinetics-how do wetting lines move?," in *AIChE international symposium on the mechanics of thin-film coating, New Orleans*, 1988.

[23] G. Ström, M. Fredriksson, P. Stenius, and B. Radoev, "Kinetics of steady-state wetting," *Journal of colloid and interface science*, vol. 134, no. 1, pp. 107–116, 1990.

[24] J. E. Seebergh and J. C. Berg, "Dynamic wetting in the low capillary number regime," *Chemical engineering science*, vol. 47, no. 17-18, pp. 4455–4464, 1992.

[25] M. Bracke, F. De Voeght, and P. Joos, "The kinetics of wetting: the dynamic contact angle," in *Trends in Colloid and Interface Science III*, pp. 142–149, Springer, 1989.

[26] E. Rillaerts and P. Joos, "The dynamic contact angle," *Chemical Engineering Science*, vol. 35, no. 4, pp. 883–887, 1980.

[27] K. Ishimi, H. Hikita, and M. Esmail, "Dynamic contact angles on moving plates," *AIChE journal*, vol. 32, no. 3, pp. 486–492, 1986.

[28] Z. Shi, Y. Zhang, M. Liu, D. A. Hanaor, and Y. Gan, "Dynamic contact angle hysteresis in liquid bridges," *Colloids and Surfaces A: Physicochemical and Engineering Aspects*, vol. 555, pp. 365–371, 2018.

[29] P. Lambert *et al.*, "Surface tension in microsystems," *Engineering Below the Capillary Length*, 2013.

[30] R. L. Hoffman, "A study of the advancing interface. i. interface shape in liquid—gas systems," *Journal of colloid and interface science*, vol. 50, no. 2, pp. 228–241, 1975.

[31] T.-S. Jiang, O. Soo-Gun, and J. C. Slattery, "Correlation for dynamic contact angle," *Journal of colloid and interface science*, vol. 69, no. 1, pp. 74–77, 1979.

[32] A. Siebold, M. Nardin, J. Schultz, A. Walliser, and M. Oppliger, "Effect of dynamic contact angle on capillary rise phenomena," *Colloids and surfaces A: Physicochemical and engineering aspects*, vol. 161, no. 1, pp. 81–87, 2000.

[33] P. A. Thompson and M. O. Robbins, "Simulations of contact-line motion: slip and the dynamic contact angle," *Physical review letters*, vol. 63, no. 7, p. 766, 1989.

[34] M. Reiner, *Ten lectures on theoretical rheology*. R. Mass, 1943.

[35] A. Einstein, *Eine neue bestimmung der molekü ldimensionen*. PhD thesis, ETH Zurich, 1905.

[36] I. E. Zarraga, D. A. Hill, and D. T. Leighton Jr, "The characterization of the total stress of concentrated suspensions of noncolloidal spheres in newtonian fluids," *Journal of Rheology*, vol. 44, no. 2, pp. 185–220, 2000.

[37] J. Chong, E. Christiansen, and A. Baer, "Rheology of concentrated suspensions," *Journal of applied polymer science*, vol. 15, no. 8, pp. 2007–2021, 1971.

[38] I. M. Krieger, "Rheology of monodisperse latices," *Advances in Colloid and Interface science*, vol. 3, no. 2, pp. 111–136, 1972.

[39] S. H. Maron and P. E. Pierce, "Application of ree-eyring generalized flow theory to suspensions of spherical particles," *Journal of colloid science*, vol. 11, no. 1, pp. 80–95, 1956.

[40] J. Y. Moon, *A study on filament breakup process of silicone oil/PMMA suspensions*. PhD thesis, Seoul National University, 2016.

[41] I. M. Krieger and T. J. Dougherty, "A mechanism for non-newtonian flow in suspensions of rigid spheres," *Transactions of the Society of Rheology*, vol. 3, no. 1, pp. 137–152, 1959.

[42] J. Happel and H. Brenner, *Low Reynolds number hydrodynamics: with special applications to particulate media*, vol. 1. Springer Science & Business Media, 2012.

[43] W. R. Schowalter, *Mechanics of non-newtonian fluid*. Pergamon, 1978.

국문초록

유변특성 평가를 통한 잉크젯 공정 안정화 방안

진 용 현
응용공학과 응용공학전공
서울대학교 공학전문대학원

최근 디스플레이 제품은 소비자의 니즈를 반영하여 더 얇고 더 커질 뿐만 아니라 화면을 구부리거나 접는 등 제품 형태도 다양화되고 있습니다. 이러한 고객의 요구를 만족시키기 위해 최신 기술이 적용된 고가의 장비를 사용하여 제품을 생산함에 따라 제품의 생산 원가가 점차 증가하고 있습니다. 이에 디스플레이 산업체들은 경쟁사 대비 생산원가 경쟁력을 갖기 위해 생산 라인에 대체 기술을 도입하여 기존 고가의 생산 공정을 저비용 공정으로 개선하려고 노력하고 있습니다. 디스플레이 제품 중 OLED[1] 제품 생산에서 가장 개선이 필요한 부분은 증착 공정으로, 특수장비 유지 보수비용 및 유기재료의 낭비가 많아 개선이 절실한 상황입니다. 이에 업계에서는 증착 공정을 대체할 기술로 잉크젯 프린팅을 주목하고 있으며, 잉크젯 기술 적용시 생산 원가를 50% 이상 절감 할 수 있습니다. 이와 같은 이유로 개발자들은 잉크젯 프린팅을 도입하기 위해 특수 잉크를 개발하고 독자적으로 프린팅 장비를 제작하고 있지만, 표준화된 규격이나 공정 기준이 없기 때문에 공정 안정화 및 양산 개발에 많은 어려움이 있습니다.

본 연구에서는 이러한 어려움을 해결하기 위해, 잉크의 유변학적 특성을 기준으로 잉크젯 프린팅 공정의 안정화 방안을 찾는 것을 목표로 연구 하였습니다.

[1] Organic Light Emitting Diode

공정 결과가 현탁액의 유변 특성에 따라 달라진다는 사실에 초점을 맞춰, 다양한 페인트의 유변 특성과 슬라이드 코팅된 샘플의 접촉각 사이의 상관 관계를 분석하는 실험을 진행하였습니다. 그 결과 유변학 특성 중 점도가 증가함에 따라 공정결과인 접촉각이 증가하는 것을 확인하였습니다. 그리고 다양한 크기의 PMMA[2] 입자를 부피비율에 따라 실리콘 오일에 분산시킨 현탁액을 제조하여 유변 특성을 분석한 실험결과, 입자의 부피 분율을 조정하면 유변학 특성인 점도를 조절할 수 있는 것을 확인 하였습니다. 또한 입자 부피분율을 15%까지 상승 시키면 점도값을 100%까지 증가시킬 수 있음을 실험으로 증명 하였습니다.

이러한 공정결과를 유변학적 특성으로 예측할 수 있다는 점에 착안하여 잉크의 유변특성, 공정 결과, 장비 설정값 간의 관계를 연결한 잉크젯 공정 안정화 방법론을 제시하였으며, 이를 통해 회사의 잉크젯 공정 SOP[3]를 수립 할 수 있는 기반을 마련 하였습니다.

주요어 : 잉크젯프린팅, 공정 안정화 방안, 유변특성 평가, 점도/접촉각, 실리콘오일/PMMA 현탁액

학번 : 2019-26873

[2]Poly methyl methacrylate
[3]Standard Of Procedure

Thanks to

2019년 따뜻한 봄날, 회사 생활 10여년만에 학교로 돌아와 공부할 수 있는 소중한 기회를 얻었습니다. 낯설기만 했던 학교 생활도 이제 마무리 해야 하는 시간이 되었지만, 다시 강의실 칠판을 보며 학업에 집중했던 시간이 제 인생의 값진 추억으로 남았습니다.

연구실에 받아주시고, 연구 지도를 위해 힘써주신 안경현 지도교수님께 감사 드립니다. 공전원에서 지도를 해주신 김화용 교수님, 정광섭 교수님께 감사 드립니다. 그리고 유변 실험하는데 많은 도움을 준 미세유변학 연구실 연구원들께 고맙다고 마음 전합니다.

다시 공부할 수 있도록 배려해주신 센터장님, 팀장님, 동료 분들께 감사 드립니다. 함께 해서 즐거웠던 공전원 4기 여러분들 오래 봤으면 좋겠습니다. 건강하시고 자주 연락 드릴게요.

항상 믿어주시고 묵묵히 지켜봐 주신 아버지, 어머니 사랑하고 존경합니다. 부모님의 사랑과 가르침으로 이렇게 성장할 수 있었습니다.

마지막으로 사랑하는 나의 아내 최자은에게 다시 공부하는 남편을 이해해주고, 항상 심려 깊게 물심양면으로 응원해 줘서 고맙다고 마음을 전합니다. 그리고 아들 진선우와 함께 항상 행복한 하루를 만들어 줘서 고맙다고 말로 표현할 수 없는 마음을 전합니다. 사랑합니다.

지나고 보니 모두 다 추억입니다.

2021년 2월 진용현 드림.